ACS Catalysis

Letter

pubs.acs.org/acscatalysis

Enantioselective Synthesis of 1-Aryl-Substituted Tetrahydroisoquinolines Employing Imine Reductase

Jinmei Zhu,[†] Hongqun Tan,[†] Lu Yang,[†] Zheng Dai,[†] Lu Zhu,[†] Hongmin Ma,[†] Zixin Deng,[†] Zhenhua Tian,[‡] and Xudong Qu*[,†,§]

[†]Key Laboratory of Combinatorial Biosynthesis and Drug Discovery, Ministry of Education, School of Pharmaceutical Sciences, Wuhan University, Wuhan 430071, China

[‡]Shanghai R&D Center, Abiochem Co., Ltd., 1299 Ziyue Road, Minhang District, Shanghai 200241, China

[§]Jiangsu National Synergetic Innovation Center for Advanced Materials (SICAM), Nanjing 211816, Jiangsu, China

Supporting Information

ABSTRACT: Tetrahydroisoquinolines (THIQs) with a C1-aryl-substituted groups are common in many natural and synthetic compounds of biological importance. Currently, their enantioselective synthesis are primarily reliant on chemical catalysis. Enzymatic synthesis using imine reductase is very attractive, because of the cost-effectiveness, high catalytic efficiency, and enantioselectivity. However, the steric hindrance of the 1-aryl substituents make this conversion very challenging, and current successful examples are mostly restricted to the simple alkyl-THIQs. In this report, through extensive evaluation of a large collection of IREDs (including 88 enzymes), we successfully identified a panel of steric-hindrance tolerated IREDs. These enzymes are able to convert *meta*- and *para*-substituted chloro-, methyl-, and methoxyl-benzyl dihydroisoquinolines (DHIQs) into corresponding *R*- or *S*- THIQs with very high enantioselectivity and conversion. Among them, the two most hindrance-tolerated enzymes (with different stereospecificity) are also able to convert *ortho*-substituted chloro-, methyl-, and methoxyl-benzyl DHIQs and dimethoxyl 1-chlorobenzyl-DHIQs with good enantiometric excess. Furthermore, using *in silico* modeling, a highly conserved tryptophan residue (W191) was identified to be critical for substrate accommodation in the binding cavity of the *S*-selective IRED (IR45). Replacing W191 with alanine can dramatically increase the catalytic performance by decreasing the K_m value by 2 orders of magnitude. Our results provide an effective route to synthesize these important classes of THIQs. Moreover, the disclosed sequences and substrate binding model set a solid basis to generate more-efficient and broad-selective enzymes via protein engineering.

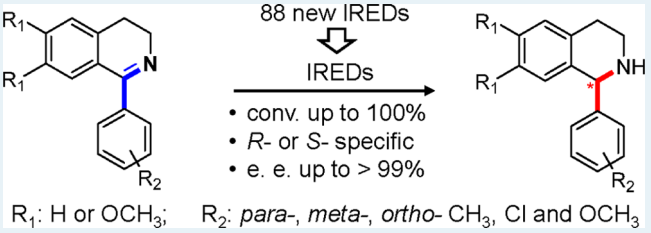

KEYWORDS: *biocatalysis, imine reductase, tetrahydroisquinolines, hindrance tolerated IRED, solifenacin*

Tetrahydroisoquinolines (THIQs) are a class of important molecular scaffolds common in natural products and biological active molecules.[1,2] Compounds with this moiety often possess a remarkable spectrum of bioactivities, such as multidrug resistance reversal, antidiabetic properties, bradycardia, and central nervous system (CNS) activities.[2−4] Therefore, efficient incorporation of THIQs has become an important synthetic strategy in drug discovery.[1−4] Within this class of compounds, the 1-aryl substituted products are of particular interest, because of their broad spectrum of biological activities and significant pharmaceutical properties.[5,6] The representative molecules **I**, **II**, and solifenacin (**III**) (Figure 1), have been used as drug candidates and medicine for neurological disorders,[7] leukemia treatment,[8] and clinical treatment of overactive bladder syndrome,[9,10] respectively.

To date, synthetic efforts have been extensively devoted to the development of efficient methods for THIQs synthesis.[1,2] However, despite the high catalytic efficiency of chemical catalysis,[1,2] their enantioselectivity and cost remains a challenge

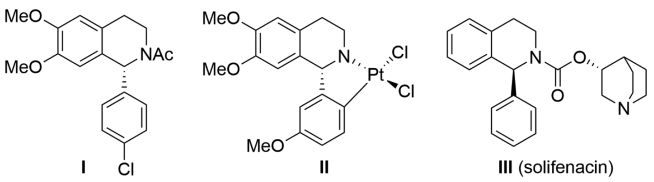

Figure 1. Selected bioactive 1-aryl-THIQs. **I**, **II**, and **III** (solifenacin) are representative compounds of pharmaceutical interest or clinical use.

for industrial application.[1,2,11] Therefore, additional cost-effective approaches, especially through biocatalysis, are highly welcomed. Recently, the application of artificial imine reductases (IREDs),[12] norcoclaurine synthase,[13,14] monoamine oxidase,[15−17] reductive aminase,[18] and IREDs[19−27] have been

Received: August 5, 2017
Revised: September 9, 2017
Published: September 15, 2017

DOI: 10.1021/acscatal.7b02628
ACS Catal. 2017, 7, 7003−7007

Scheme 1. Asymmetric Reduction of 1-Benzyl-DHIQ Derivatives by IREDs

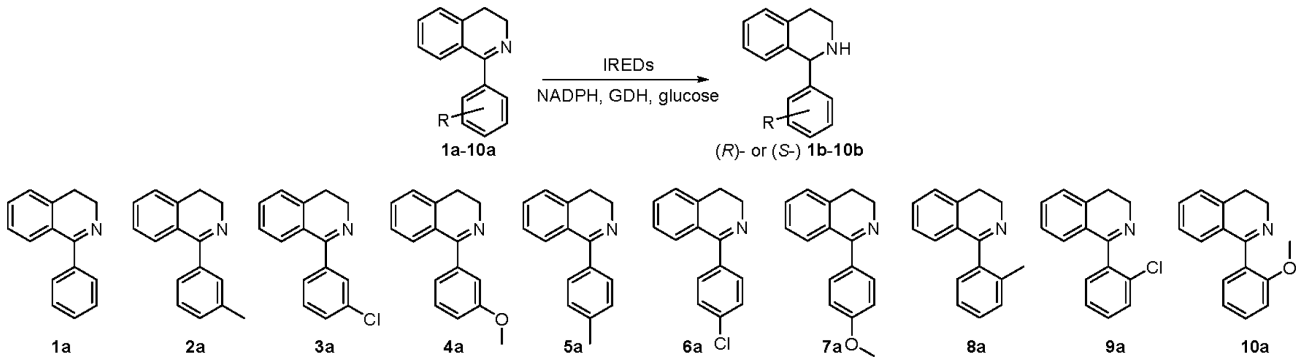

Table 1. Conversion and Enantioselectivity of Selected IREDs toward 1a−10a

	Conversion (%) and Enantiometric Excess (ee) (%)[a]									
substance	IR2	IR8	IR17	IR19	IR20	IR32	IR45	IR71	IR96	IR99
1a	100; 96^{R}	99; >99^{R}	100; >99^{R}	99; >99^{R}	99; >99^{R}	99; >99^{R}	99; >**99**^{S}	7; 30^{R}	78; **90**^{S}	97; **97**^{S}
2a	99; >99^{R}	99; >99^{R}	99; >99^{R}	100; >99^{R}	100; 99^{R}	100; >99^{R}	99; >**99**^{S}	4; 84^{R}	29; 47^{R}	24; 16^{R}
3a	100; 99^{R}	100; 97^{R}	100; >99^{R}	99; >99^{R}	100; >99^{R}	99; 98^{R}	99; **91**^{S}	47; 58^{R}	74; 81^{R}	50; **21**^{S}
4a	100; >99^{R}	100; >99^{R}	100; >99^{R}	99; >99^{R}	100; >99^{R}	100; >99^{R}	99; >**99**^{S}	26; 19^{R}	26; **8**^{S}	16; 2^{R}
5a	100; >99^{R}	99; >99^{R}	99; > 99^{R}	99; >99^{R}	99; >99^{R}	99; >99^{R}	100; **35**^{S}	94; 72^{R}	46; 97^{R}	24; 91^{R}
6a	99; >99^{R}	99; >99^{R}	99; >99^{R}	100; >99^{R}	100; >99^{R}	99; >99^{R}	79; 36^{R}	82; **3**^{S}	52; 95^{R}	27; 34^{R}
7a	100; >99^{R}	99; >99^{R}	100; >99^{R}	100; >99^{R}	99; >99^{R}	99; >99^{R}	5; **21**^{S}	28; 93^{R}	4; 97^{R}	5; 93^{R}
8a	36; >99^{R}	0	0	0	0	0	7; **26**^{S}	0	0	0
9a	23; **5**^{S}	0	0	0	0	0	9; >99^{R}	0	0	0
10a	5; >99^{R}	0	0	0	0	0	8; 98^{R}	0	0	0

[a]First value shown represents conversion, and the second value represents the ee value. Stereospecificity are indicated by the superscripts; ee values shown in bold indicate *S*-configuration. All reactions were performed at 30 °C for 24 h.

successfully developed for the synthesis of THIQs. Among of them, employing IREDs to asymmetrically reduce dihydroisoquinolines (DHIQs) is particularly attractive. These enzymatic routes are cost-effective and generally able to afford very high enantioselectivity.[28] However, because of the strong steric hindrance of aryl substituents in C1, which affects enzyme activity, these studies are mostly restricted to 1-alkyl substituted THIQs.[19−26] The only successful attempt to access 1-aryl-THIQ was very recently reported using the IRED *Sn*IR, which converts the imine substrate (**1a**, Scheme 1) into *S*-1-phenyl-THIQ (*S*-**1b**) with a moderate enantiometric excess (ee) value (51%).[27] Consideration of the poor stereoselectivity and limited substrate scope of *Sn*IR, additional enzymes with more broad specificity and higher catalytic efficiency and stereoselectivity are desired. To solve this bottleneck, we herein performed extensive exploration of the sequence space of IREDs. Through systematically exploring the activity of a large collection of IREDs (88 new entities), we successfully identified a group of highly hindrance-tolerated enzymes that can efficiently convert a series of methyl-, chloro-, and methoxyl-substituted 1-phenyl-DHIQs and 6,7-diomethoxyl-DHIQ into the corresponding aryl-THIQs with high enantioselectivity and conversion.

To identify the sequence that can accept model substrate 1-phenyl-DHIQ (**1a**), we initially examined a small collection of five IREDs (IR4, IR26, IR71, IR82, IR97; see the Supporting Information), which previously have been demonstrated to efficiently convert the 1-methyl-DHIQ into 1-methyl-THIQ.[22,25] These proteins were assayed for the asymmetric reduction activity of the **1a**. One enzyme IR71 shows clear activity (Table 1), although the conversion (7%) and enantioselectivity (*R*-selective, 30% ee) are modest. By using IR71 as bait, a large collection of homologous proteins were further identified from the Imine Reductase Engineering Database.[29] To ensure the collection contains adequately diverse specificity, proteins with high amino acid identity to each other were excluded. Based on these criteria, a total of 95 novel IREDs were identified (Table S1 in the Supporting Information) including 68 *R*-type (IR1−IR3, IR5−IR25, IR27−IR70) and 27 *S*-type (IR72−IR81, IR83−IR96, IR98−IR100) IREDs (classified based on the residue in 187, according to ref 29). Genes encoding these novel IREDs were synthesized based on the codon bias of *Escherichia coli* and cloned into pET28a for overexpression. Evaluation of their expression in *E. coli* revealed that most proteins were well expressed in the supernatant; 7 IREDs (IR10, IR23, IR67, IR73, IR84, IR85, IR86) formed inclusion bodies (Figure S1 in the Supporting Information) and were excluded from further studies.

The soluble IREDs (88 novel entities) were subsequently employed to assay of the model substrate **1a** based on the UV-vis absorbance of NADPH in 340 nM. Compound **1a** was generally a poor substrate for most of the enzymes, with only 10 enzymes (IR2, IR8, IR17, IR19, IR20, IR32, IR45, IR96, and IR99, as well as the initially identified IR71) exhibiting obvious activities. Further evaluation of the substrate conversions by HPLC (Table 1) revealed that (i) all the new enzymes except for IR96 (78% conversion) show very good activity, leading to almost complete conversion (97%−100%); (ii) IR2, IR8, IR17, IR19, IR20, IR32 are *R*-specific and IR45, IR96, IR99 are *S*-specific. These two groups exhibit very good stereoselectivity with ee values ranging from 97% to >99%, except for the IR96 (ee = 90%). Interestingly, unlike other *R*-type IREDs (IR2, IR8,

DOI: 10.1021/acscatal.7b02628
ACS Catal. 2017, 7, 7003−7007

Table 2. Kinetics Parameters of Selected IREDs

	IR2			IR17			IR45		
substrate	K_m (mM)	k_{cat} (s^{-1})	k_{cat}/K_m (s^{-1} mM^{-1})	K_m (mM)	k_{cat} (s^{-1})	k_{cat}/K_m (s^{-1} mM^{-1})	K_m (mM)	k_{cat} (s^{-1})	k_{cat}/K_m (s^{-1} mM^{-1})
1a	0.026	1.54	59.23	0.19	0.52	2.73	0.17	0.32	1.88
2a	0.048	1.48	30.83	0.59	5.93	10.05	0.11	0.33	3.00
3a	0.024	9.57	398.75	0.019	2.09	110.00	0.031	0.041	1.32
4a	0.029	1.54	53.10	0.12	0.71	5.91	0.11	0.034	0.31
5a	0.022	3.65	166.91	0.047	1.40	29.78	ND[a]	ND[a]	ND[a]
6a	0.023	11.29	490.87	0.069	1.00	14.49	ND[a]	ND[a]	ND[a]

[a]Not determined.

IR17, IR19, IR20, IR32) IR45 shows a complete reversed stereospecificity. The performance of IR45 (99% conversion and >99% ee) and IR97 (97% conversion and 97% ee) are particularly attractive as their product *S*-**1b** is the pivot intermediate of solifenacin (Figure 1). Further analysis of the kinetic parameters of IR45 and the two other most active *R*-selective IREDs (IR2 and IR7) revealed that their catalytic efficiency are, indeed, quite efficient (k_{cat}/K_m = 1.88, 59.23, and 2.73 s^{-1} mM^{-1}, respectively) (see Table 2). Moreover, both IR45 and IR17 show no obvious or strong substrate inhibition effect (no inhibition for IR17; weak inhibition for IR45, Figures S2B and S2C in the Supporting Information), which makes them very suitable for large-scale production. To demonstrate the practical utility of these enzymes, preparative-scale biotransformations of **1a**−**7a** by IR2, IR8, IR17, and IR45 were performed on a 5 mM scale. The complete conversion with 91.2%−96.5% isolated yields and >99% ee of *S*-**1b**−*S*-**7b** (Table S2 in the Supporting Information) confirms their potential for practical application.

The ability to accept benzyl group in the C1 position of DHIQ led us to further evaluate their potential to convert substituted-benzyl DHIQs. Representative substituents, including methyl, chloro, and methoxyl groups in the *meta*- and *para*-position of 1-benzyl-DHIQ (**2a**−**7a**, Scheme 1) were prepared and assayed. Of significance, IR2, IR8, IR17, IR19, IR20, IR32 exert both excellent conversion (>99%) and stereoselectivity (ee > 99%) of the six *meta*- and *para*-substituted benzyl-DHIQs to the corresponding *R*-substituted benzyl-THIQs (*R*-**2b**−*R*-**7b**) (see Table 1). Contrary to the *R*-type, the *S*-type IREDs (IR71, IR96, and IR99) show very diverse conversion of these substrates. Even more, their stereospecificities are mostly reversed to the *R*-configuration and only in a few cases show *S*-specificity with poor ee values (3%−21%) (see Table 1). These results indicate that IREDs, including both of *R*- and *S*-types, naturally prefer to produce *R*-isomers of substituted-benzyl THIQs. It is very interesting that IR45 retains the *S*-specificity to most substrates, especially for the *meta*-substituted benzyl-DHIQs, with very high conversion (99%) and *S*-specificity (ee values between 91% and >99%) (Table 1). For the *para*-substituted methyl and methoxyl benzyl-DHIQs, IR45 resulted in a low-to-medium *S*-selectivity (ee = 20.9%−35%), and only reversed to *R*-selectivity when the *para*-substituted chlorobenzyl-DHIQ is employed (ee = 36%). The activity of IR45 is influenced by the size of the *para*-substituted groups (decrease from methyl and chloro to methoxyl), suggesting the existence of steric hindrance in the binding pocket (see below). Finally, the kinetic parameters of IR45 and the two other most active *R*-selective IREDs (IR2 and IR7) were characterized, which confirmed that these proteins are indeed highly efficient to substrates **2a**−**6a** (see Table 2). The identification of efficient IREDs, particularly, the rare *S*-specific IR45, is very important and can provide an efficient and cost-effective avenue to generate enantio-pure substituted benzyl-THIQs.

The good tolerance to the steric hindered *meta*-, *para*-substituted benzyl-DHIQs by these enzymes, led us further interested in their conversion of more challenging substrates, for instance, the *ortho*-substituted-benzyl DHIQs. Three representative methyl-, chloro-, and methoxyl-substituted benzyl-DHIQs (**8a**−**10a**; see Scheme 1) were prepared and assayed by the aforementioned 10 IREDs. Although most of the IREDs are completely inactive to these substrates, IR2 and IR45 are still able to convert them, with a conversion ranging from 5% to 36% (see Table 1). The stereoselectivity of these reactions were generally very high (ee values between 98% and >99%), with the exception of **9a** by IR2 (ee = 5%) and **8a** by IR45 (ee = 26%) generated in low optical purity (see Table 1). IR45 keeps the *S*-specificity to methyl-substituted substrate (**8a**) and reversed to *R*-specificity for the chloro, methoxyl, benzyl-DHIQs (**9a** and **10a**). The reversed stereospecificity toward *ortho*-chloronated, methoxylated, and *para*-chloronated substrates (also see **11a** below) is interesting, and may result from the both of the steric hindrance and electrostatic effects between substrate and residues in the catalytic cavity. In addition to the 1-aryl group, some pharmaceutically interesting THIQs also have methoxyl groups in the C6 and C7 (Figure 1).[2] The methoxyl groups increase both of the steric hindrance and electron density, which can reduce the imine reactivity, thus are even more challenging for enzyme reduction. Currently, no results have been reported to convert 1-aryl dimethoxyl-THIQs by IREDs. To test the activity of our enzymes for these types of substrates, the model substrate *p*-chlorobenzyl-6,7-dimethoxyl-DHIQ (**11a**) was prepared and assayed by the 10 previously mentioned IREDs (IR2, IR8, IR17, IR19, IR20, IR32, IR45, IR71, IR96, and IR99). As anticipated, most of the enzymes are completely inactive to this highly sterically hindered substrate. Interestingly, the two most tolerated substrates, IR2 and IR45, can still convert it to *R*-**11b** with a medium conversion (62% and 53%, respectively) and high stereoselectivity (ee = 99% for IR2 and 92% for IR45) (see Scheme 2). *R*-**11b** is a pharmaceutically important intermediate,[7] and these enzymes provide a simple and efficient route for its synthesis. Both IR2 and IR45 can accommodate diverse substituents in the 1-benzyl group (*meta*-, *ortho*-, and *para*-positions); hence, it is also expected for them to convert other dimethoxyl substituted-benzyl DHIQs. The broad tolerance to steric hindrance of IR2 and IR45 provides a biocatalytic route to access very steric-hindered aryl-THIQs, and their sequence is a good starting point to create more efficient and stereospecific IREDs via protein engineering.

Finally, the distinct stereospecificity of IR45 from other *R*-type IREDs led us to analyze their mode of recognition. Consistent with their specificity, IR2, IR8, IR17, IR19, IR20,

DOI: 10.1021/acscatal.7b02628
ACS Catal. 2017, 7, 7003−7007

Scheme 2. Asymmetric Reduction of *p*-Chlorobenzyl-6,7-dimethoxyl-DHIQ (11a) by IR2 and IR45

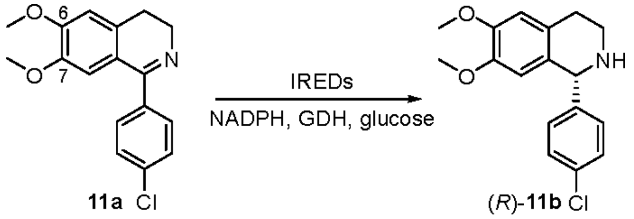

IR2: 62% conv., 99% e.e; **IR45**: 53% conv., 92% e.e

and IR32 are phylogenetically close to each other. The identity between them ranges from 70% to 80%, while their identity to IR45 is only ~39%. To correlate these difference to the substrate specificity, the structures of IR2 and IR45 were modeled based on the *R*-type IRED Q1EQE0 (Figure S3 in the Supporting Information),[30] which is 44% and 64%, identical to the IR2 and IR45, respectively. Docking **1a** into the binding pocket of IR45 revealed that the substrate is closely surrounded by the conserved aspartic acid (D183) and NADPH, which fits the catalytic model of nucleophilic addition by NADPH and protonation by D183 (Figure 2).[30] Moreover, the benzyl group

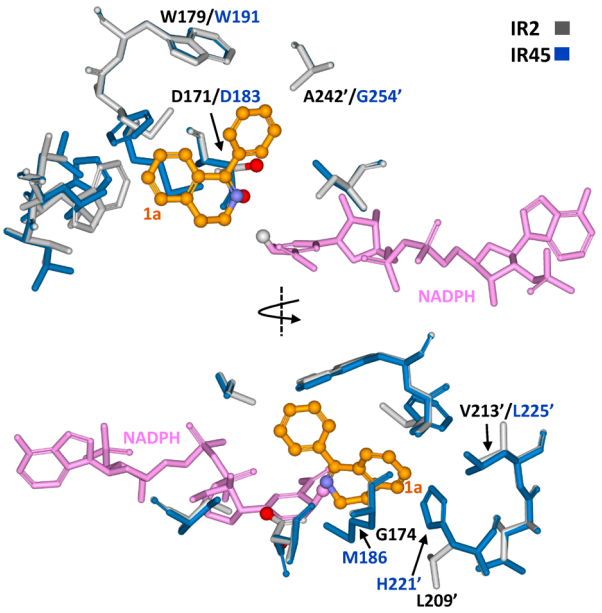

Figure 2. An in silico model of IR2 and IR45 with substrate **1a**. The structures of IR2 (gray) and IR45 (indigo blue) are modeled based on Q1EQE0 (PDB: 3zhb)[30] and docked with **1a** (yellowish brown) and NADPH (pink); critical residues in the binding cavity are labeled by corresponding amino acids; residues from chain B are indicated by quotation marks. To clearly show the catalytic dyad, both of the proton-donating hydroxyl group (red) of aspartic acid (D171/183) and hydrogen atom (gray) of the NADPH are highlighted in round shape.

of **1a** is pointing to the upper left cavity, which is constituted by the W191 of subunit A and G254′ of subunit B. This orientation presents the molecule to the Si face of NADPH and subsequently yields the *S*-product. Interestingly, superimposing IR2 onto IR45 revealed some distinct features:

(i) Residues M186 (chain A), and H221′ and L225′ (chain B) in the IR45 are replaced by smaller residues G174, L209′, V213′ in IR2, which forms a large cavity in the upper right region.

(ii) The G254′ in IR45 was replaced by alanine (A242′) in IR2, which can cause a steric hindrance to the phenyl group of the substrate (1.6 Å).

These differences together force the benzyl group of **1a** to reside in the upper right cavity and expose the Re face to the NADPH and to generate the *R*-products in IR2. It is interesting that the residues constituting the upper left cavity in most IREDs are W or Y (corresponding to 191 in IR45) and A or S (corresponding to 254′ in IR45) (see Figure S4 in the Supporting Information), which could be too bulky to accommodate the substituted benzyl-THIQs. This may explain the reason why the natural preference of IREDs to substituted benzyl-THIQs are mostly *R*-specific. In IR45, the upper left cavity is composed by the W191 and the smallest residue G254′; to further expand its space, W191 was changed to L and A, respectively. Kinetic analysis of the resulting mutants IR45-W191L and IR45-W191A revealed that the K_m values of both mutants are dramatically decreased, particularly for the W191A, whose K_m value is 2 orders of magnitude (170 fold) lower than the wild-type IR45 (see Table 3). This result confirmed its

Table 3. Kinetics Parameters of IR45 and Its Mutants in the Conversion of 1a

enzyme	K_m (mM)	k_{cat} (s^{-1})	k_{cat}/K_m (s^{-1} mM^{-1})
IR45	0.17	0.32	1.88
IR45-W191L	0.027	0.013	0.48
IR45-W191A	0.001	0.015	15.00

critical role in substrate accommodation in the upper left binding cavity. In addition, the decreased k_{cat} value also indicated this conserved residue is important for maintenance of the protein confirmation. Further evaluation of other mutations in this position may be able to identify more balanced mutants. The overall catalytic efficiency (k_{cat}/K_m) of W191A is ~8-fold better than the wild-type IR45 (Table 3); moreover, substrate inhibition in W191A was completely eliminated, compared to the wild-type IR45 (K_i = 2.81 mM) (see Figures S2C and S7B in the Supporting Information), making this mutant even more efficient for practical application. The identification of the significant W191 provides a promising way to expand (by engineering) the scope of *S*-specific 1-aryl-DHIQs processing IREDs. Currently, engineering the upright binding cavities of IR2 is also in progress to improve the performance and expand its substrate scope.

In summary, through identification and evaluation of a large collection of new IREDs (88 novel IREDs), a panel of steric-hindrance-tolerated IREDs with high catalytic efficiency and stereospecificity toward 1-ary-THIQs has been identified. These enzymes are able to efficiently convert *para*- and *meta*-substituted methyl-, chloro-, and methoxyl-phenyl DHIQs into corresponding THIQ products with high conversion and enantioselectivity (both of *R*- and *S*-, up to >99% ee). To the most challenging substrates, including *ortho*-substituted phenyl-DHIQs and diomethoxyl chloro-benzyl-DHIQ, both IR45 and IR2 maintain activity with good enantioselectivity in most cases. The practical application of IR45 to generate the solifenacin intermediate *S*-**1b** was demonstrated via preparative-scale synthesis, providing a cost-effective solution to its current resolution-based production way.[11] Finally, the highly conserved residue W191 was identified to be critical for substrate

DOI: 10.1021/acscatal.7b02628
ACS Catal. 2017, 7, 7003−7007

accommodation. By introducing a smaller residue (Ala) in the position, the catalytic efficiency of IR45 can be increased by 8-fold. These results open a door for further improving IREDs catalytic performance and creating other *S*-specific enzymes via protein engineering. Moreover, the number of new IREDs (88 novel IREDs) disclosed in this study is almost twice the sum of previously identified IREDs, which expands our knowledge and toolbox of IREDs enormously. Our work not only provides enzymatic solutions to synthesize these important class of THIQs but also the sequence basis for unraveling the unusual substrate specificity of IREDs to further generate more-efficient enzymes via protein engineering.

■ ASSOCIATED CONTENT

Supporting Information

The Supporting Information is available free of charge on the ACS Publications website at DOI: 10.1021/acscatal.7b02628.

Methods providing general materials and methods; synthesis, cloning, expression, and purification of IREDs; activity screening; biotransformation; determination of kinetic constants; chiral HPLC analysis; imine substrates and racemic amine synthesis; in silico modeling and docking; supplementary tables providing IREDs information; isolated yield of preparative reactions; HPLC columns and conditions used for the chiral analysis of the biotransformation products; kinetic parameters (with errors) of IR2, IR17, and IR45 toward imine; kinetic parameters (with errors) of IR45 and its mutants at W191; supplementary figures providing SDS-PAGE analysis of IRED; determination of kinetic constants; in silico models of IR2 and IR45 based on the template of Q1EQE0; partial sequence alignment of IR1−IR100; HPLC analysis of the enzyme conversion; chiral HPLC analysis of the enantioselectivity; kinetic data, and NMR spectra (PDF)

■ AUTHOR INFORMATION

Corresponding Author

*E-mail: quxd@whu.edu.cn.

ORCID

Xudong Qu: 0000-0002-3301-8536

Notes

The authors declare no competing financial interest.

■ ACKNOWLEDGMENTS

This work was financially supported by the NSFC (Nos. 31322002, 31270119). We thank Wenbo Liu in the College of Chemistry, Wuhan University for providing the help of chiral analysis.

■ REFERENCES

(1) Liu, W.; Liu, S.; Jin, R.; Guo, H.; Zhao, J. *Org. Chem. Front.* **2015**, *2*, 288−299.

(2) Chrzanowska, M.; Grajewska, A.; Rozwadowska, M. D. *Chem. Rev.* **2016**, *116*, 12369−12465.

(3) Perez, M.; Wu, Z.; Scalone, M.; Ayad, T.; Ratovelomanana-Vidal, V. *Eur. J. Org. Chem.* **2015**, *2015*, 6503−6514.

(4) Singh, I. P.; Shah, P. *Expert Opin. Ther. Pat.* **2017**, *27*, 17−36.

(5) Wu, Z.; Perez, M.; Scalone, M.; Ayad, T.; Ratovelomanana-Vidal, V. *Angew. Chem., Int. Ed.* **2013**, *52*, 4925−4928.

(6) Li, D.; Yang, D.; Wang, L.; Liu, X.; Wang, K.; Wang, J.; Wang, P.; Liu, Y.; Zhu, H.; Wang, R. *Chem. - Eur. J.* **2017**, *23*, 6974−6978.

(7) Gitto, R.; Barreca, M. L.; De Luca, L.; De Sarro, G.; Ferreri, G.; Quartarone, S.; Russo, E.; Constanti, A.; Chimirri, A. *J. Med. Chem.* **2003**, *46*, 197−200.

(8) von Nussbaum, F.; Miller, B.; Wild, S.; Hilger, C. S.; Schumann, S.; Zorbas, H.; Beck, W.; Steglich, W. *J. Med. Chem.* **1999**, *42*, 3478−3485.

(9) Naito, R.; Yonetoku, Y.; Okamoto, Y.; Toyoshima, A.; Ikeda, K.; Takeuchi, M. *J. Med. Chem.* **2005**, *48*, 6597−6606.

(10) Abrams, P.; Andersson, K.-E. *BJU Int.* **2007**, *100*, 987−1006.

(11) Ji, Y.; Shi, L.; Chen, M.-W.; Feng, G.-S.; Zhou, Y.-G. *J. Am. Chem. Soc.* **2015**, *137*, 10496−10499.

(12) Köhler, V.; Wilson, Y. M.; Dürrenberger, M.; Ghislieri, D.; Churakova, E.; Quinto, T.; Knörr, L.; Häussinger, D.; Hollmann, F.; Turner, N. J.; Ward, T. R. *Nat. Chem.* **2012**, *5*, 93−99.

(13) Lichman, B. R.; Zhao, J.; Hailes, H. C.; Ward, J. M. *Nat. Commun.* **2017**, *8*, 14883.

(14) Erdmann, V.; Lichman, B. R.; Zhao, J.; Simon, R. C.; Kroutil, W.; Ward, J. M.; Hailes, H. C.; Rother, D. *Angew. Chem., Int. Ed.* **2017**, in press (DOI: 10.1002/anie.201705855).

(15) Ghislieri, D.; Green, A. P.; Pontini, M.; Willies, S. C.; Rowles, I.; Frank, A.; Grogan, G.; Turner, N. J. *J. Am. Chem. Soc.* **2013**, *135*, 10863−10869.

(16) Li, G.; Yao, P.; Gong, R.; Li, J.; Liu, P.; Lonsdale, R.; Wu, Q.; Lin, J.; Zhu, D.; Reetz, M. T. *Chem. Sci.* **2017**, *8*, 4093−4099.

(17) Foulkes, J. M.; Malone, K. J.; Coker, V. S.; Turner, N. J.; Lloyd, J. R. *ACS Catal.* **2011**, *1*, 1589−1594.

(18) Aleku, G. A.; France, S. P.; Man, H.; Mangas-Sanchez, J.; Montgomery, S. L.; Sharma, M.; Leipold, F.; Hussain, S.; Grogan, G.; Turner, N. J. *Nat. Chem.* **2017**, in press (DOI: 10.1038/nchem.2782).

(19) Leipold, F.; Hussain, S.; Ghislieri, D.; Turner, N. J. *ChemCatChem* **2013**, *5*, 3505−3508.

(20) Huber, T.; Schneider, L.; Präg, A.; Gerhardt, S.; Einsle, O.; Müller, M. *ChemCatChem* **2014**, *6*, 2248−2252.

(21) Hussain, S.; Leipold, F.; Man, H.; Wells, E.; France, S. P.; Mulholland, K. R.; Grogan, G.; Turner, N. J. *ChemCatChem* **2015**, *7*, 579−583.

(22) Wetzl, D.; Berrera, M.; Sandon, N.; Fishlock, D.; Ebeling, M.; Müller, M.; Hanlon, S.; Wirz, B.; Iding, H. *ChemBioChem* **2015**, *16*, 1749−1756.

(23) Maugeri, Z.; Rother, D. *Adv. Synth. Catal.* **2016**, *358*, 2745−2750.

(24) Aleku, G. A.; Man, H.; France, S. P.; Leipold, F.; Hussain, S.; Toca-Gonzalez, L.; Marchington, R.; Hart, S.; Turkenburg, J. P.; Grogan, G.; Turner, N. J. *ACS Catal.* **2016**, *6*, 3880−3889.

(25) Scheller, P. N.; Nestl, B. M. *Appl. Microbiol. Biotechnol.* **2016**, *100*, 10509−10520.

(26) Man, H.; Wells, E.; Hussain, S.; Leipold, F.; Hart, S.; Turkenburg, J. P.; Turner, N. J.; Grogan, G. *ChemBioChem* **2015**, *16*, 1052−1059.

(27) Li, H.; Tian, P.; Xu, J.-H.; Zheng, G.-W. *Org. Lett.* **2017**, *19*, 3151−3154.

(28) Grogan, G.; Turner, N. J. *Chem.—Eur. J.* **2016**, *22*, 1900−1907.

(29) Scheller, P. N.; Fademrecht, S.; Hofelzer, S.; Pleiss, J.; Leipold, F.; Turner, N. J.; Nestl, B. M.; Hauer, B. *ChemBioChem* **2014**, *15*, 2201−2204.

(30) Rodríguez-Mata, M.; Frank, A.; Wells, E.; Leipold, F.; Turner, N. J.; Hart, S.; Turkenburg, J. P.; Grogan, G. *ChemBioChem* **2013**, *14*, 1372−1379.

DOI: 10.1021/acscatal.7b02628
ACS Catal. 2017, 7, 7003−7007